

Appendix A

Procedures for Monitoring in a Few Commercial Systems

The main monitoring tool addressed here is the Schottky plot. At the end we will briefly address the recording of (part of) the facet emission pattern in the Quanta 200F scanning electron microscope (SEM).

Key to useful Schottky plot data from commercial systems are creating a field-free zone between the extractor and the beam-defining aperture (or at least zero lens effect), and making the beam path free from obstructions from the beam-defining aperture to the entrance aperture of a Faraday cup on the stage.

The apertures that can be used as beam-defining apertures for Schottky plot recording are for the:

NOVA NanoSEM: the 2nd extractor aperture (acceptance half-angle 3.45 mrad)

Quanta 3D FEG: the aperture after the C0 lens (acceptance half-angle 1.99 mrad)

Quanta 200F: the decelerating lens aperture (acceptance half-angle 1.34 mrad)

For the Quanta 200F the zone between the extractor and the beam-defining aperture can be made field free by turning off the C1 and C2 lenses. The objective lens is then used to focus the beam into the Faraday cup aperture.

For the Quanta 3D FEG the zone between the extractor and the beam-defining aperture can be made field free by turning off the C0 lens. For both the NOVA NanoSEM and the Quanta 3D FEG, to ensure a free beam path beyond the beam-defining aperture, the C1 and C2 lenses are used to make crossovers, with the C2 lens crossover

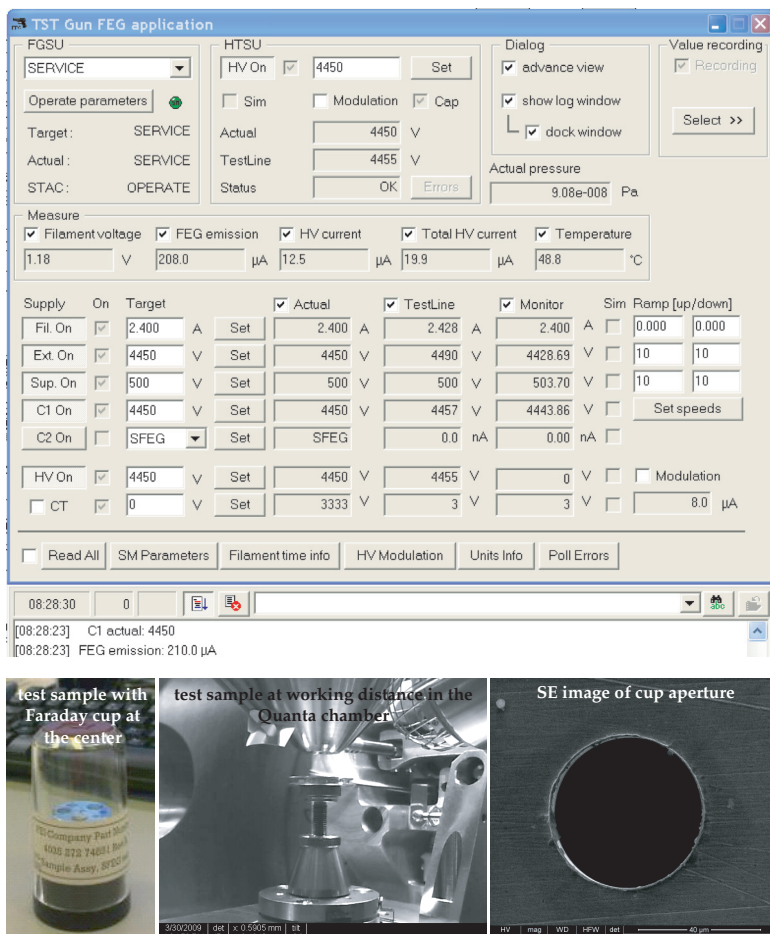
onto the decelerating lens aperture. Note that when the extraction voltage is changed, the lens effect between the extractor and the C1 lens is also changed. It may be required, for each data point, to manually optimize the settings of the condenser system (C1 C2) to get all current through the decelerating lens aperture.

A.1 Recording Schottky Plots in Quanta 3D FEG and NOVA NanoSEM Systems

- Log on as “support” so that you are allowed to change the voltage settings of the electron gun.
- Vent the chamber.
- Put a Faraday cup on the stage (e.g., the one on a standard FEI* test sample).
- Free the beam path:
 - Remove the “insert” from the objective lens, if present, and leave the “insert” inside chamber (check the manual; use the designated tool).
 - Change to the largest aperture on the strip (1 mm diameter).
- Connect the Faraday cup to a current meter.
- Pump down the chamber.
- Bring the stage to a working distance.
- Change the configuration in “8_system configuration” to high vacuum mode.
- Quanta 3D FEG: go to spot 4.0, 10 kV beam energy; NOVA NanoSEM: go to spot 6.0 (the condenser systems of these machines are calibrated to give a focus on the decelerating lens aperture for these settings).
- Switch on the beam.
- Optimize the crossover position.
- Focus on the aperture of the Faraday cup in “quad 1” (top-left window).
- Go to the TstEGun window. Check the “advance view” box, if not checked.

*FEI Beam Technology Division, 5350 NE Dawson Creek Dr, Hillsboro, OR 97124, USA.

- Write down any relevant parameter values (date, system, heating current, heating voltage, gun pressure, total emission current, Coulomb tube (CT) current, extraction voltage, suppressor voltage, C1 lens setting, etc.).
- Turn off the beam.
- Change the operating mode from OPERATE to SERVICE. (N.B. The software Software can return a message, which you can “hide”).
- Check the C1 lens voltage. Set it at the same value as it was in the OPERATE mode, if it has changed.
- Turn the beam on by pressing “HV on” in the TstEGun window (either of the two buttons).
- Change the ramping speeds for suppressor and extractor voltage from 0 V to 10 V for both up and down. Press “set speeds” to confirm.
- Go from scan mode to spot mode and put the spot inside the aperture.
- Write down V_{ext} (“Actual” value), V_{sup} (“Actual” value), I_{total} (FEG emission), I_{cup} (current meter), and the time in a table.
 1. Change from spot mode to scan mode.
 2. Reduce V_{ext} with 100 V.
 3. Change V_{sup} proportional to the V_{ext} change. This is to maintain the same field form around the tip (e.g., going from a 5.0 kV and 500 V to a 4.9 kV extraction voltage requires a suppressor voltage of $4.9/5.0 \times 500$ V).
 4. Go to spot mode and put the beam inside the cup (optional: check that the crossover position is still optimal).
 5. Write down V_{ext} , V_{sup} , I_{total} , I_{cup} , and the time in the table.
- Repeat the above five steps for the desired number of voltage settings. Check at one of the lower extraction voltages if the crossover is still looking OK and if all of the beam still goes into the Faraday cup.
- Bring back the settings to the settings of OPERATE mode.
- Beam off.
- Bring the extractor and the suppressor voltage back to the settings of OPERATE mode (see the top part of your filled out source monitoring work sheet). **Wait until the values are set.**



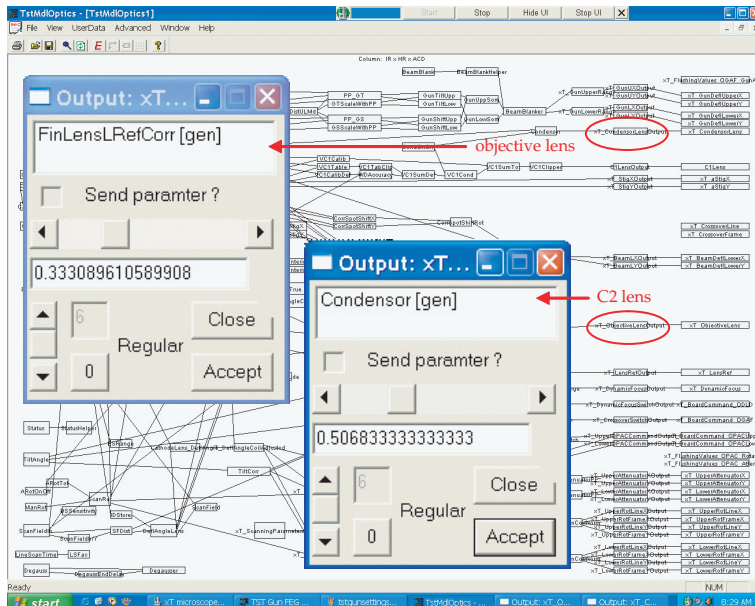
- Change ramping speeds of the extraction and the suppressor voltage from 10 to 0 (do not forget to press “set speeds”).
- Change from SERVICE mode to OPERATE mode.
- Set back the aperture number from 1 mm to what it was before the measurement.
- Beam on and check the system by imaging something at high resolution.
- Beam off.
- Vent the chamber.
- Take out the Faraday cup.

- Put the “insert” back into the objective lens.
- Check Part III on the source monitoring sheet.
- Pump the chamber.
- Set the system configuration back from “high vacuum mode” to the setting that belongs to the “insert.”
- Log off.
- Analyze the data and extract the field enhancement factor. Has it changed with respect to the last time, and what is the field strength the source is operating at?

Recording Schottky plots in the Quanta 200F system:

- Log on as “support” to be able to change the voltage settings.
- Vent the chamber.
- Put a Faraday cup on the stage (e.g., the standard FEI test sample).
- Free the beam path:
 - Remove the “insert” from the objective lens, if present (see the manual), and leave the “insert” inside the chamber.
 - Check if the blunker is present? Set it to the largest separation: setting 4.
 - Change to the largest aperture on the strip (number 1, 1 mm diameter).
- Connect the Faraday cup to a current meter.
- Pump down the chamber.
- Bring the stage to a working distance.
- Switch on the beam.
- Set the source tilt to zero.
- Focus on the aperture of the Faraday cup in “quad 1” (top-left window).
- Go to the TstEGun window. Check the “advance view” box.
- Write down any relevant parameter values (date, system, heating current, heating voltage, total emission current, CT current, extraction voltage, suppressor voltage, etc.).
- Turn off the beam.
- Change the operating mode to SERVICE. (N.B. The software returns a message, which you can “hide”).
- Turn the beam on by pressing “HV on” in the TstEGun window (either of the two buttons).

- Change the ramping speeds for the suppressor and the extractor voltage to 10 V for both up and down. Press “set speeds.”
- Turn off the CT (clear the box) (means it goes to ground potential).
- Change V_{C1} in the “Target” column to the V_{ext} value (press the set button or use Enter to confirm) (N.B. By doing this the potential on the C1 lens becomes zero with respect to ground).
- Change HV in the “Target” column to the V_{ext} value (press the set button or use Enter to confirm) (N.B. By doing this the potential on the extractor becomes zero with respect to ground).
- Go to the TstEOptics window. Open the xT_ObjectiveLensOutput window (objective/final lens) and the xT_CondenserLensOutput window (C2 lens).



- Set the condenser lens excitation (C2 lens) to zero. Watch the image of the Faraday cup aperture and adjust the objective lens setting if you start to lose track of the hole.
- If necessary focus a little bit by optimizing the objective lens setting.

- Go from scan mode (full frame) to spot mode and put the spot inside the aperture.
- Check the current meter reading to make sure all current is going into the cup.
- Check if the alignment of the aperture on the stick is such that all current passes it: do this by changing its alignment and monitor the current reading from the cup and maximize it.
- Write down V_{ext} ("Actual" value), V_{sup} ("Actual" value), I_{total} (FEG emission), I_{CT} (bottom right in the TstEGun window), I_{cup} (current meter), and the time in a table.
 1. Change from spot mode to scan mode.
 2. Reduce V_{ext} with 100 V.
 3. Change V_{sup} proportional to the V_{ext} change. This is to maintain the same field form around the tip (e.g., going from a 5.0 kV and 500 V to a 4.9 kV extraction voltage requires a suppressor voltage of $4.9/5.0 \times 500$ V).
 4. Set V_{C1} to the same value as the extractor.
 5. Set HV to the same value as the extractor.
 6. Set the condenser lens excitation to zero.
 7. If necessary focus a little bit on the aperture with the objective lens.
 8. Go to spot mode and put the beam inside the cup.
 9. Write down V_{ext} , V_{sup} , I_{total} , I_{CT} , I_{cup} , and the time in a table.
- Repeat the above nine steps for the desired number of voltage settings.
- Turn off the beam.
- Bring back the extractor and the suppressor voltage to the settings of OPERATE mode (see the top part of your filled out source monitoring work sheet). **Wait until the values are set.**
- Change ramping speeds of the extraction and the suppressor voltage from 10 to 0 (do not forget to press "set speeds").
- Change from SERVICE mode to OPERATE mode.
- Set back the aperture number from 1 to what it was before the measurement.
- Beam on and check the system by making a high-resolution image.
- Beam off.

- Vent the chamber.
- Take out the Faraday cup.
- Put the “insert” back into the objective lens, if required.
- Pump the chamber.
- Log off.
- Analyze the data and extract the field enhancement factor. Has it changed with respect to the last time, and what is the field strength the source is operating at?

A.2 Imaging of the Facet in the Quanta 200F System

The Quanta 200F extractor accepts part of the total facet beam: its acceptance half-angle is ~ 66 mrad (3.8°). If the C1 lens is turned off (same voltage as the extractor) or collimates the beam, the beam intensity profile in the CT behind the C1 lens is part of the facet emission pattern.

The intensity profile of the beam in the CT can be measured by scanning the beam across the CT aperture by using “gun tilt” and collecting the current through the aperture in a Faraday cup on the stage.

The gun tilt can be changed manually in the TstEOptics menu under “Gun tilt,” with a maximum range of -1 to 1 for both *x* and *y*. The “Gun tilt” setting determines which part of the beam is selected by the CT aperture. This is done by changing the settings of the two sets of deflector plates, which are positioned somewhere along the CT. Because there are two sets of deflectors the pivot point can be maintained at the same height. This is done automatically when changing the gun tilt.

The divergence or collimation of the facet beam leaving the extractor can be tuned by changing the spot number (which changes the C1 lens setting): the part of the beam that is scanned by changing the gun tilt settings increases with increasing spot number. If the beam diameter at the CT aperture becomes smaller than the aperture size the recorded image will start showing the shadow image of the extractor aperture.

Appendix B

Procedure to Characterize System Performance

The performance of a probe-forming system can be characterized if the following parameters are available:

Source: practical brightness, FW50 energy spread, extraction voltage, virtual source size ($B, \Delta E, V_{\text{ext}}, d_v$)

Column: spherical and chromatic aberration coefficients of the final lens (C_s, C_c)

Gun: spherical and chromatic aberration coefficients of the gun lens (C_{sg}, C_{cg})

Target: beam energy (V_p)

Key is which probe size contributions are dominant at the desired probe current level?

Approach: Calculate the parameters below and follow the scheme to find (1) which probe size contributions are dominant for your system at the probe current of interest, (2) the optimum probe size, (3) the associated half opening angle of the beam, and (4) the magnification of the virtual source.

$$\text{Calculate } I_{AI} = 1.08 \cdot 10^{-18} B \quad (I \text{ for which } d_A = d_l)$$

$$\text{Calculate } \delta_{CA} = 1.99 \cdot 10^{-5} \sqrt{C_c \frac{\Delta E}{V_p^{3/2}}} \quad \text{and} \quad \delta_{SA} = 8.46 \cdot 10^{-8} \left(\frac{C_s}{V_p^{3/2}} \right)^{1/4}$$

$$\text{Calculate } I_{AC_g} = 2.72 \cdot 10^{-9} \frac{BV_{\text{ext}}^{3/2} d_v^2}{C_{cg} \Delta E} \quad \text{and} \quad I_{AS_g} = 1.50 \cdot 10^{-4} \frac{BV_{\text{ext}}^{3/4} d_v^2}{C_{sg}^{1/2}} \\ (I \text{ for which } d_A = d_{cg}) \quad (I \text{ for which } d_A = d_{sg})$$

Calculate $I_{ICg} = \frac{I_{ACg}^2}{I_{AI}}$ and $I_{ISg} = \left(\frac{I_{ASg}^2}{\sqrt{I_{AI}}} \right)^{2/3}$
 I for which $d_I = d_{Sg}$

Is the desired probe current below I_{AI} ?

$\delta_{CA} > \delta_{SA}$: d_C balances d_A $\rightarrow d_p$ from Table B.1; α and M from
 $\delta_{CA} < \delta_{SA}$: d_S balances d_A Table B.2

Is the desired probe current between I_{AI} and the smallest of (I_{ISg}, I_{ICg})?

$\delta_{CA} > \delta_{SA}$: d_C balances d_I $\rightarrow d_p$ from Table B.1; α and M from
 $\delta_{CA} < \delta_{SA}$: d_S balances d_I Table B.2

Is the desired probe current larger than the smallest of (I_{ISg}, I_{ICg})?

$I_{ICg} > I_{ISg}$:
 $\delta_{CA} > \delta_{SA}$: d_C balances d_{Sg} $\rightarrow d_p$ from Table B.1; α and M from
 $\delta_{CA} < \delta_{SA}$: d_S balances d_{Sg} Table B.2

$I_{ICg} < I_{ISg}$:

desired probe current smaller than I_{CgSg} ?

$\delta_{CA} > \delta_{SA}$: d_C balances d_{Cg} $\rightarrow d_p$ from Table B.1; α and M from
 $\delta_{CA} < \delta_{SA}$: d_S balances d_{Cg} Table B.2

desired probe current larger than I_{CgSg} ?

d_{Cg} balances d_{Sg} $\rightarrow d_p$ from Table B.1; α and M from Table B.2

Table B.1 Optimum total probe size d_p for the desired probe current for a balance between d_A , d_I , d_{Cg} or d_{Sg} and d_C or d_S . Also given is the figure of merit (fm) for column and source

	d_C		d_S			
	d_p (m)	fm column	fm source	d_p (m)	fm column	fm source
d_A	$\sqrt{2}\delta_{CA}$	$\frac{1}{C_C}$	$\frac{1}{\Delta E}$	$1.15\delta_{SA}$	$\frac{1}{C_S}$	-
d_I	$\sqrt{2}\delta_{CA} \left(\frac{I}{I_{AI}} \right)^{1/4}$	$\frac{1}{C_C}$	$\frac{B}{\Delta E^2}$	$1.54\delta_{SA} \left(\frac{I}{I_{AI}} \right)^{3/8}$	$\frac{1}{C_S}$	B

d_c		d_s			
d_p (m)	fm column	fm source	d_p (m)	fm column	fm source
\mathbf{d}_{cg}	$\delta_{CA} \left(\frac{I}{I_{ACg}} \right)^{1/2}$	$\frac{1}{C_C C_{cg}}$	$\frac{V_{ext}^{3/2} Bd_v^2}{\Delta E^2}$	$\sqrt{2} \delta_{SA} \left(\frac{I}{I_{ACg}} \right)^{3/4}$	$\frac{1}{C_S C_{cg}^{3/4}}$
\mathbf{d}_{sg}	$\sqrt{2} \delta_{CA} \left(\frac{I}{I_{ASg}} \right)^{1/2}$	$\frac{1}{C_C C_{sg}}$	$\frac{V_{ext}^{3/4} Bd_v^2}{\sqrt{\Delta E}}$	$1.75 \delta_{SA} \left(\frac{I}{I_{ASg}} \right)^{3/2}$	$\frac{1}{C_S C_{sg}^{3/4}}$

Table B.2 Optimum magnification of the virtual source, M , and optimum half opening angle of the beam at the target, $\alpha_{p,opt}$, for different regimes in which two balancing contributions dominate the total probe size

d_c		d_s	
M	$\alpha_{p,opt}$ (rad)	M	$\alpha_{p,opt}$ (rad)
\mathbf{d}_A	-	$\frac{6.62 \cdot 10^{-10}}{\sqrt{V_p} \delta_{CA}}$	-
\mathbf{d}_I	$\sqrt{2} \frac{d_p}{d_v}$	$\frac{6.62 \cdot 10^{-10}}{\sqrt{V_p} \delta_{CA}} \left(\frac{I}{I_{AI}} \right)^{1/4}$	$0.80 \frac{d_p}{d_v}$
\mathbf{d}_{cg}	$\left(\frac{C_C}{C_{cg}} \right)^{1/2} \left(\frac{V_g}{V_p} \right)^{3/4}$	$\frac{6.62 \cdot 10^{-10}}{\sqrt{V_p} \delta_{CA}} \left(\frac{I}{I_{ACg}} \right)^{1/2}$	$\frac{\delta_{SA} I_{ACg}^{1/4}}{d_v \sqrt{I_{AI}}} I^{1/4}$
\mathbf{d}_{sg}	$\frac{\delta_{CA}}{d_v} \frac{I_{ASg}}{\sqrt{I_{AI}}} \frac{1}{\sqrt{I}}$	$\frac{6.62 \cdot 10^{-10}}{\sqrt{V_p} \delta_{CA}} \left(\frac{I}{I_{ASg}} \right)^{1/1}$	$\left(\frac{C_S}{C_{sg}} \right)^{1/4} \left(\frac{V_g}{V_p} \right)^{3/8}$
			$\frac{6.62 \cdot 10^{-10}}{\sqrt{V_p} \delta_{SA}} \left(\frac{I}{I_{ASg}} \right)^{1/2}$

Bibliography

1. S. Babin, M. Gaevsky, D. Joy, M. Machin, A. Martynov, *J. Vac. Sci. Technol. B*, **24** (2006), 2956.
2. A. S. Bahm, G. A. Schwind, L. W. Swanson, *J. Vac. Sci. Technol. B*, **26** (2008), 2080.
3. J. P. Barbour, F. M. Charbonnier, W. W. Dolan, W. P. Dyke, E. E. Martin, J. K. Trolan, *Phys. Rev.*, **117** (1960), 1452.
4. J. E. Barth, P. Kruit, *Optik*, **101** (1996), 101.
5. J. E. Barth, M. D. Nykerk, *Nucl. Instrum. Methods, Phys. Res. A*, **427** (1999), 86.
6. A. E. Bell, L. W. Swanson, *Phys. Rev. B*, **19** (1979), 3353.
7. K. Besocke, H. Wagner, *Phys. Rev. B*, **8** (1973), 4597.
8. K. Besocke, B. Krahl-Urban, H. Wagner, *Surf. Sci.*, **68** (1977), 39.
9. P. C. Bettler, G. G. Love, *J. Appl. Phys.*, **38** (1967), 3835.
10. P. C. Bettler, G. Barnes, *Surf. Sci.*, **10** (1968), 165.
11. P. C. Bettler, D. H. Bennum, C. M. Case, *Surf. Sci.*, **44** (1974), 360.
12. H. Boersch, *Z. Phys.*, **139** (1954), 115.
13. C. Bombis, A. Emundts, M. Nowicki, H. P. Bonzel, *Surf. Sci.*, **511** (2002), 83.
14. H. P. Bonzel, *Phys. Rep.*, **385** (2003), 1.
15. A. S. Carasso, D. S. Bright, A. E. Vladár, *Opt. Eng.*, **41** (2002), 2499.
16. S. P. Chen, *Surf. Sci. Lett.*, **274** (1992), L619.
17. S. G. Christov, *Phys. Status Solidi*, **17** (1966), 11.
18. *Charged Particle Optics*, <http://www.electronoptics.com>.
19. A. C. Crewe, in *Handbook of Charged Particle Optics*, edited by J. Orloff (CRC, New York, 1997), Chap. 10, p. 406.

20. U. Dahmen, R. Erni, V. Radmilovic, C. Kisielowski, M.D. Rossell, P. Denes, *Philos. Trans. R. Soc. A*, **367** (2009), 3795.
21. L. R. Danielson, L. W. Swanson, *Surf. Sci.*, **88** (1979), 14.
22. L. R. Danielson, *J. Appl. Phys.*, **52** (1981), 6769.
23. M. Degawa, K. Thürmer, E. D. Williams, *Phys. Rev. B*, **74** (2006a), 155432.
24. M. Degawa, K. Thürmer, E. D. Williams, *Jpn. J. Appl. Phys.*, **45** (2006b), 2070.
25. A. K. Dokania, J. F. M. Velthuis, Y. Zhang, P. Kruit, *J. Vac. Sci. Technol. B*, **25** (2007), 504.
26. A.K. Dokania, M. Pelle, P. Kruit, *Microelectron. Eng.*, **85** (2008), 1031.
27. W. P. Dyke, F. M. Charbonnier, R. W. Strayer, R. L. Floyd, J. P. Barbour, J. K. Trolan, *J. Appl. Phys.*, **31** (1960), 790.
28. A. B. El-Kareh, J. C. Wolfe, J. E. Wolfe, *J. Appl. Phys.*, **48** (1977), 4749.
29. A. Ferriere, L. Lestrange, J-F. Robert, *J. Solar Energy Eng.*, **122** (2000), 9.
30. J. H. Fink, B. W. Schumacher, *Nucl. Instrum. Methods*, **130** (1975), 353.
31. R. G. Forbes, *J. Vac. Sci. Technol. B*, **26** (2008), 788.
32. M. J. Fransen, E. P. N. Damen, C. Schiller, T. L. van Rooy, H. B. Groen, P. Kruit, *Appl. Surf. Sci.*, **94–95** (1996), 107.
33. M. J. Fransen, J. S. Faber, T. L. van Rooy, P. C. Tiemeijer, P. Kruit, *J. Vac. Sci. Technol. B*, **16** (1998), 2063.
34. M. J. Fransen, T.L. de Rooy, P. C. Tiemeijer, M. H. F. Overwijk, J. S. Faber, P. Kruit, *Adv. Imag. Electron Phys.*, **111** (1999), 91.
35. M. J. Fransen, M. H. F. Overwijk, P. Kruit, *Appl. Surf. Sci.*, **146** (1999), 357.
36. S. Fujita, H. Shimoyama, *J. Electron Microsc.*, **54** (2005), 331.
37. S. Fujita, H. Shimoyama, *J. Electron Microsc.*, **54** (2005), 413.
38. S. Fujita, H. Shimoyama, *J. Vac. Sci. Technol. B*, **24** (2006), 1891.
39. S. Fujita, H. Shimoyama, *Phys. Rev. B*, **75** (2007), 235431.
40. G. Fursey, in *Field Emission in Vacuum Microelectronics*, edited by I. Brodie, P. Shwoebel, (Kluwer Academic/Plenum Publishers, New York, 2005), Chap. 7, p. 115.
41. M. Gesley, *J. Vac. Sci. Technol. B*, **9** (1991), 2949.
42. M. Giesen, G. Schulze Icking-Konert, H. Ibach, *Phys. Rev. Lett.*, **80** (1998), 552.
43. M. Giesen, *Prog. Surf. Sci.*, **68** (2001), 1.

44. M. Giesen, G. Beltramo, S. Dieluweit, J. Müller, H. Ibach, W. Schmickler, *Surf. Sci.*, **595** (2005), 127.
45. J. B. McGinn, S. G. den Hartog, D. S. Jun, G. G. Magera, G. A. Schwind, United States Patent 6680562 B1 (2004).
46. R. Gomer, L. W. Swanson, *J. Chem. Phys.*, **38** (1963), 1613.
47. D. J. Griffiths, *Introduction to Quantum Mechanics* (2nd ed.) (Prentice Hall, 2004), Chap. 8, p. 315.
48. G. A. Haas, in *The American Institute of Physics Handbook*, 3rd ed., edited by D. E. Gray (McGraw-Hill, 1972), pp. 9-172–9-186.
49. P. W. Hawkes, E. Kasper, *Principles of Electron Optics*, Vol. 2 (Academic Press, London, 1996), Chap. 47, p. 971.
50. P. W. Hawkes, E. Kasper, *Principles of Electron Optics*, Vol. 2 (Academic Press, London, 1996), Chap. 44, p. 924.
51. C. Herring, M. H. Nichols, *Rev. Mod. Phys.*, **21** (1949), 185.
52. C. Herring, in *The Physics of Powder Metallurgy*, edited by W. E. Kingston (McGraw-Hill, New York, 1951), Chap. 8, p. 143.
53. N. Hirai, K. Watanabe, S. Hara, *Surf. Sci.*, **493** (2001), 568.
54. M. Horn-Von Hoegen, F.-J. Meyer zu Heringdorf, D. Kähler, T. Schmidt, E. Bauer, *Thin Solid Films*, **336** (1998), 16.
55. W. Hu, X. Shu, B. Zhang, *Comput. Mater. Sci.*, **23** (2002), 175.
56. A. R. Hutson, *Phys. Rev.*, **98** (1955), 889; G. F. Smith, *Phys. Rev.*, **100** (1955), 1115.
57. H. Ibach, W. Schmickler, *Phys. Rev. Lett.*, **91** (2003), 016106.
58. H. Ibach, *Physics of Surfaces and Interfaces*, (Springer-Verlag, Berlin, Heidelberg, 2006), Chap. 4, p. 149.
59. A. Ichimiya, K. Hayashi, E. D. Williams, T. L. Einstein, M. Uwaha, K. Watanabe, *Appl. Surf. Sci.*, **175-176** (2001), 33.
60. Y. Irokawa, R. Mitsuhashi, S. Lee, K. Min, M. Inoue, Y. Kimura, R. Shimizu, *Jpn. J. Appl. Phys.*, **35** (1996), 4042.
61. N. Israeli, D. Kandel, *Phys. Rev. B*, **60** (1999), 5946.
62. S. C. Jain, V. Sinhas, B. K. Reddys, *J. Phys. D: Appl. Phys.*, **3** (1970), 1359.
63. G. H. Jansen, *Adv. Electron. Electron Phys.*, (Suppl. 21) (1990).
64. X. R. Jiang, P. Kruit, *Microelectron. Eng.*, **30** (1996), 249.
65. X. R. Jiang, *Coulomb Interactions in Charged Particle Optical Columns* (PhD thesis, Delft University of Technology, 1996), ISBN 90-407-1369-3.

66. N. de Jonge, *J. Appl. Phys.*, **95** (2004), 673.
67. D. C. Joy, *J. Microsc.*, **208** (2002), 24.
68. D. C. Joy, in *Characterization and Metrology for ULSI Technology 2005: Richardson, Texas, 15-18 March 2005*, edited by D. G. Seiler, Paper no. CP 788, (American Institute of Physics, Melville, 2005), p. 535.
69. N. K. Kang, D. Tuggle, L. W. Swanson, *Optik*, **63** (1983), 313.
70. H. Kawano, *Prog. Surf. Sci.*, **83** (2008), 1.
71. E. C. Kemble, *Phys. Rev.*, **48** (1935), 549.
72. H. S. Kim, M. L. Yu, E. Kratschmer, B. W. Hussey, M. G. R. Thomson, T. H. P. Chang, *J. Vac. Sci. Technol. B*, **13** (1995), 2468.
73. H. S. Kim, M. L. Yu, M. G. R. Thomson, E. Kratschmer, T. H. P. Chang, *J. Vac. Sci. Technol. B*, **15** (1997), 2284.
74. H. S. Kim, M. L. Yu, M. G. R. Thomson, E. Kratschmer, T. H. P. Chang, *J. Appl. Phys.*, **81** (1997), 461.
75. W. Knauer, *Optik*, **59** (1981), 335.
76. E. Kratschmer, S. A. Rishton, D. P. Kern, T. H. P. Chang, *J. Vac. Sci. Technol. B*, **6** (1988), 2074.
77. P. Kruit, M. Bezuijen, J. E. Barth, *J. Appl. Phys.*, **99** (2006), 024315.
78. P. Kruit, G. H. Jansen, in *Handbook of charged particle optics (Second Edition)*, edited by J. Orloff (CRC Press, New York, 2008), Chap. 7, p. 341.
79. M. V. Kuz'min, M. A. Mittsev, *Tech. Phys. Lett.*, **27** (2001), 437.
80. N. D. Lang, W. Kohn, *Phys. Rev. B*, **1** (1970), 4555.
81. N. D. Lang, W. Kohn, *Phys. Rev.*, **3** (1971), 1215.
82. R. R. Law, *Proc. Inst. Radio Eng.*, **25** (1937), 954.
83. S. C. Lee, Y. Irokawa, M. Inoue, R. Shimizu, *Surf. Sci.*, **330** (1995), 289.
84. J. A. Liddle, P. Naulleau, G. Schmid, *J. Vac. Sci. Technol. B*, **22** (2004), 2897.
85. D.-J. Liu, J. D. Weeks, M. D. Johnson, E. D. Williams, *Phys. Rev. B*, **55** (1997), 7653.
86. D. Liu, H. M. Lu, Q. Jiang, *J. Phys.: Condens. Matter*, **21** (2009), 198002.
87. A. Y. Lozovoi, A. Alavi, *Phys. Rev. B*, **68** (2003), 245416.
88. J. Mackenzie, A. J. W. Moore, J. F. Nicholas, *J. Phys. Chem. Solids*, **23** (1962), 185.
89. T. Matsumoto, A. Cezairliyan, D. Basak, *Int. J. Thermophys.*, **20** (1999), 943.

90. T. Matsumoto, A. Ono, G. Barreiro, paper presented at the Fourteenth Symposium on Thermophysical Properties, June 25–30, 2000, Boulder, Colorado, USA.
91. I. Merrick, J. E. Inglesfield, G. A. Attard, *Phys. Rev. B*, **72** (2005), 033403.
92. A. Modinos, *Field, Thermionic, and Secondary Electron Emission Spectroscopy*, (Plenum Press, New York, 1984), Chap. 1, p. 1.
93. A. Modinos, J. P. Xanthakis, *Surf. Sci.*, **249** (1991), 373.
94. J. Müller, H. Ibach, *Phys. Rev. B*, **74** (2006), 085408.
95. I. Müllerová, *Scan. Microsc.*, **13** (1999), 7.
96. W. W. Mullins, G. S. Rohrer, *J. Am. Ceram. Soc.*, **83** (2000), 214.
97. E. L. Murphy, R. H. Good, *Phys. Rev.*, **102** (1956), 1464.
98. Y. Neo, H. Mimura, T. Matsumoto, *Appl. Phys. Lett.*, **88** (2006), 073511.
99. F. A. Nichols, W. W. Mullins, *J. Appl. Phys.*, **36** (1965), 1826.
100. J. Orloff, L. W. Swanson, J.-Z. Li, *J. Vac. Sci. Technol. B*, **3** (1985), 224.
101. V. G. Pavlov, *Phys. Solid State*, **48** (2006), 720.
102. I. Petroff, C. R. Viswanathan, *Phys. Rev. B*, **4** (1971), 799.
103. T. Radlicka, B. Lencová, *Ultramicroscopy*, **108** (2008), 455.
104. F. H. Read, N. J. Bowring, *Rev. Sci. Instrum.*, **74** (2003), 2280.
105. F. H. Read, N. J. Bowring, *Nucl. Instrum. Methods A*, **519** (2004), 196.
106. L. Reimer, *Scanning Electron Microscopy: Physics of Image Formation and Microanalysis* (Springer, Berlin, 1998), Chap. 2, p. 53.
107. S. A. Rishton, S. P. Beaumont, C. D. W. Wilkinson, *J. Phys. E: Sci. Instrum.*, **17** (1984), 296.
108. A. M. Rodriguez, G. Bozzolo, J. Ferrante, *Surf. Sci.*, **289** (1993), 100.
109. S. Sakawa, K. Tsunoda, Y. Terui, *Surf. Interface Anal.*, **35** (2003), 11.
110. N. Samoto, R. Shimizu, H. Hashimoto, N. Tamura, K. Gamo, S. Namba, *Jpn. J. Appl. Phys.*, **1**, **24** (1985), 766.
111. G. A. Schwind, D. S. Jun, G. G. Magera, United States Patent 6798126 B2, 2004.
112. G. A. Schwind, G. Magera, L. S. Swanson, *J. Vac. Sci. Technol. B*, **24** (2006), 2897.
113. H. Shimoyama, S. Maruse, *Ultramicroscopy*, **15** (1984), 239.
114. V. N. Shrednik, V. G. Pavlov, A. A. Rabinovich, B. M. Shaikhin, *Phys. Status Solids A*, **23** (1974), 373.
115. J. A. Simpson, *Rev. Sci. Instrum.*, **32** (1961), 1283.

116. H. L. Skriver, N. M. Rosengaard, *Phys. Rev. B*, **46** (1992), 7157.
117. D. F. Stafford, A. H. Weber, *J. Appl. Phys.*, **34** (1963), 2667.
118. *Surface Explorer*, <http://surfexp.fhi-berlin.mpg.de/>.
119. L. W. Swanson, G. A. Schwind, in *Handbook of Charged Particle Optics*, edited by J. Orloff (CRC Press, New York, 1997), Chap. 2, p. 77.
120. L. W. Swanson, G. A. Schwind, in *Handbook of Charged Particle Optics (Second Edition)*, edited by J. Orloff (CRC Press, New York, 2008), Chap. 1, p. 1.
121. A. Szczepkowicz, R. Bryl, *Surf. Sci.*, **559** (2004), L169.
122. M. Takeguchi, M. Morikawa, C. Hanqing, R. Shimizu, K. Tsunoda, H. Hagiwara, H. Hiraoka, *Technol. Rep. Osaka Univ.*, **41** (1991), 267.
123. K. Tamura, M. Amano, W. Chu, H. Ishii, M. Owari, T. Kawano, T. Nagatomi, Y. Takai, C. Oshima, R. Shimizu, Y. Nihei, *Surf. Interface Anal.*, **37** (2005), 217.
124. H. Tanaka, H. Nakayama, K. Watanabe, *Jpn. J. Appl. Phys.*, **44** (2005), 7518.
125. S. Tanaka, N. C. Bartelt, C. C. Umbach, R. M. Tromp, J. M. Blakely, *Phys. Rev. Lett.*, **78** (1997), 3342.
126. M. G. R. Thomson, *J. Vac. Sci. Technol. B*, **12** (1994), 3498.
127. K. Thürmer, J. E. Reutt-Robey, E. D. Williams, *Surf. Sci.*, **537** (2003), 123.
128. J. K. Trolan, J. P. Barbour, E. E. Martin, W. P. Dyke, *Phys. Rev.*, **100** (1955), 1646.
129. D. W. Tuggle (PhD thesis, Oregon Graduate Center, 1984).
130. M. Uwaha, *J. Phys. Soc. Jpn.*, **57** (1988), 1681.
131. A. H. V. van Veen (M.Sc. thesis, Delft University of Technology, 2000).
132. A. H. V. van Veen, C. W. Hagen, J. E. Barth, P. Kruit, *J. Vac. Sci. Technol. B*, **19** (2001), 2038.
133. L. Vitos, A. V. Ruban, H. L. Skriver, J. Kollár, *Surf. Sci.*, **411** (1998), 186.
134. A. E. Vladár, Z. Radi, M. T. Postek, D. C. Joy, *Scanning*, **28** (2006), 133.
135. W. R. Wade, *NASA-Memo-1-20-59L* (1959).
136. K. Wang, R. R. Reeber, *Mater. Sci. Eng.*, **R23** (1998), 101.
137. J. W. Ward, R. L. Kubena, M. W. Utzlaut, *J. Vac. Sci. Technol. B*, **6** (1988), 2090.
138. Y.-N. Wen, J.-M. Zhang, *Comput. Mater. Sci.*, **42** (2008), 281.
139. J. C. Wiesner, T. E. Everhart, *J. Appl. Phys.*, **44** (1973), 2140.

140. E. D. Williams, *Surf. Sci.*, **299/300** (1994), 502.
141. J. Worster, *Brit. J. Appl. Phys. (J. Phys. D)*, **2** (1969), 889.
142. W. Xu, J. B. Adams, T. L. Einstein, *Phys. Rev. B*, **54** (1994), 2910.
143. R. Young, S. Henstra, J. Chmelik, T. Dingle, A. Mangnus, G. van Veen, I. Gestmann, *Proc. SPIE*, **7378** (2009), 737803.
144. J.-M. Zhang, F. Ma, K.-W. Xu, *Surf. Interface. Anal.*, **35** (2003), 662.
145. Y. Zhang, P. Kruit, *J. Vac. Sci. Technol. B*, **25** (2007), 2239.
146. T. M. Gardiner, H. M. Kramer, E. Bauer, *Surf. Sci.*, **112** (1981) 181.

List of publications associated with this work:

- M. S. Bronsgeest, P. Kruit, *J. Vac. Sci. Technol. B*, **24** (2006), 887: "Temperature dependence of the work function of the Zr/O/W (100), Schottky electron source in typical operating conditions and its effect on beam brightness" (Section 3.5.1 of this book).
- M. S. Bronsgeest, J. E. Barth, G. A. Schwind, L. W. Swanson, P. Kruit, *J. Vac. Sci. Technol. B*, **25** (2007), 2049: "Extracting the Boersch effect contribution from experimental energy spread measurements for Schottky electron emitters" (Section 4.4.2 of this book).
- M. S. Bronsgeest, J. E. Barth, L. W. Swanson, P. Kruit, *J. Vac. Sci. Technol. B*, **26** (2008), 949: "Probe current, probe size, and the practical brightness for probe forming systems" (Section 4.2 of this book).
- M. S. Bronsgeest, P. Kruit, *J. Vac. Sci. Technol. B*, **26** (2008), 2073: "Effect of the electric field on the form stability of a Schottky electron emitter: a step model" (Section 5.5.1 of this book).
- M. S. Bronsgeest, P. Kruit, *J. Vac. Sci. Technol. B*, **27** (2009), 2524: "Reversible shape changes of the end facet on Schottky electron emitters" (Sections 5.4.2 and 5.6.1 of this book).
- M. S. Bronsgeest, P. Kruit, *Ultramicroscopy*, **110** (2010), 1243: "'Collapsing rings' on Schottky electron emitters" (Sections 5.5.2–5.6.2 of this book).

Index

- aberration coefficients 118, 215
aberrations 93, 95, 97, 99–100,
102, 110, 114, 116–17, 143
adatom 178–81, 184
adatom dipole moment 184
angular deflection 123, 126–27
angular intensity 55–58, 60, 62,
66, 75–76, 92–93, 111,
113–15, 136, 138–41,
143, 176, 208–9, 219–21,
227–29
equivalent 139–40
angular intensity distributions 50,
63, 91, 103–4, 106, 113,
144
anisotropy 153, 196
- beam
coherent 95, 108, 113
compressed 144
divergent 69
electron 3, 30, 150
large current 120
low current 120
parallel 95
primary 2
reconstructed 204, 210
beam angle 123–24
beam brightness 109
beam center 125, 128, 144–45
beam characteristics 122
beam coherence 108, 208
temporal 25
beam currents 49, 216, 221
beam-defining aperture 96–100,
103, 142, 217, 231
beam diameter 127, 238
beam direction 109
beam divergence 54, 66, 192, 212
beam edge 126
beam electrons 2, 99, 210
beam energy 33, 59–61, 109,
117–18, 239
beam envelope 123, 127
beam fluctuations 190, 224
beam instabilities 150
beam intensity distribution 109
beam intensity profile 238
beam length 127, 130, 220
beam length dependence 220
beam-limiting aperture 98, 115,
222–23, 228
beam parameters 122
beam path 119, 121, 126, 231–32,
235
beam properties 96, 144, 207–9,
216, 224, 230
final 6
intrinsic 122
beam radius 127
beam segments 122–25
cylindrical 123
beam size 127
beamlets 57, 66–67, 98, 106–8,
144–45, 208, 212
central 66, 68–69, 71–72, 74,
105–6, 108, 143, 208
multiple 145
off-axis 96, 105–8, 143–45
on-axis 105, 107
outermost 106
Boersch contribution 134, 137
Boersch effect 119–20, 122,
124–25, 128–30, 132–35,
138–41, 222

- brightness 3, 108–9, 111, 113, 118–21, 132–33, 142–43, 145, 150, 208–10, 212, 215–17, 220–21, 228–29
 equivalent 217, 220
 initial 132
 brightness definitions 112–13
 practical 109, 111
 brightness loss 119, 142–43, 220
- CCD, *see* charge-coupled device
 charge-coupled device (CCD) 34, 58, 165
 chromatic aberration 95, 137, 140, 208–9, 216, 220
 chromatic aberration coefficients 239
 circular pattern geometry 175
 cold field electron emitters 114
 cold field emission electron sources 114
 cold field emitters 26, 114–15
 collapsing planes 159–60
 collapsing rings 147–48, 150–51, 156, 177–78, 185, 188, 191–92, 198, 200–1
 collapsing Schottky emitter 148, 210
 collapsing tungsten emitters 189
 condenser lens excitation 236–37
 cone angle, smaller 74–75, 107
 cone angle emitter, small 75
 cone shape 69, 73, 213
 constant beam properties 150
 constant emitter shape 82
 constant extraction voltage 59–60, 128
 Coulomb interactions 119–21, 125, 128, 130, 132–33, 142–44, 201, 216, 222, 224
 Coulomb tube 233, 235–36, 238
 Coulomb tube aperture 238
 crystallite 151–53, 155, 168
 crystallographic orientations 5, 30, 32, 35–36, 151–52, 187, 199
 decelerating lens aperture 231–32
 diffraction 95, 110, 114, 116, 118, 217
 diffraction contributions 116, 216
 diffusion 5, 84, 179, 187–88, 229
 diffusion equations 178, 180, 187
 diffusion rates 81, 84, 176
 temperature-dependent 195
 dipoles 88–89, 180–81, 187
 bare tungsten surface 30
 positive 181, 184–85
- EELS, *see* electron energy loss spectroscopy
 electric field 3–4, 12–13, 15–17, 19, 21, 23, 25, 27, 51, 140, 153, 157, 204
 electric field energy 159
 electrodes 12–13
 electron beam equipment 2
 electron beam systems 142
 electron density 120
 electron emission 3–4, 7–8, 10, 12, 14, 16, 18, 20, 22, 24–26, 28, 38
 cold field 20
 electron emission theory 6, 114–15
 electron emitter 3
 electron energy levels 25, 81
 electron energy loss spectroscopy (EELS) 2, 25
 electron escape probability 10
 electron gun 12, 232
 electron interactions 136
 electron microscopy 108
 electron-optical system 11, 96–97, 99, 101, 103, 105, 107–8

- electron probe size 111
- electron probes 112, 116
- electron reflection 19, 89
- electron-stimulated desorption (ESD) 222
- electron wavelength 20, 113
- electron waves 11, 18
- electron-electron interactions 114, 119–21, 123, 125, 127, 129, 131, 133–35, 137, 139, 141
- electrons
 - cold 97–100, 106
 - energy distributions of 135, 142
 - fast 120
 - free 7
 - primary 3
- electrostatic lens 52
- emission
 - cone 47
 - end-facet 37
 - thermal 11
 - unstable 78
- emission calculations 14
- emission pattern 33–36, 49–50, 60–64, 81–82, 85, 88–89, 148, 165–69, 171–73, 175, 188–89, 191–93, 195–96, 199–201, 203–7
- emission properties 6, 12, 38, 49, 59–60, 69, 71–74, 76, 80, 84, 93, 227–28
- emissivity 38, 40–42, 136
 - total hemispherical 40–41
- emitter
 - collapsing 148, 189, 195
 - heated 158
 - large 221
 - larger-facet 107
 - larger-tip-size 107
 - largest 128, 133, 143, 223
 - receding 189
 - smallest 72–73, 128, 223
- spherical 189
- symmetric 61, 192
- emitter axis 199
- emitter cone 29, 42, 155, 162, 166
- emitter contour 51, 164
- emitter environment 81
- emitter extrusion 162
- emitter facet 56, 58, 161
- emitter geometry 50–51, 65, 69, 71, 73, 77, 100, 105, 107, 125, 130, 132–33, 173, 176, 215
- emitter gun geometry 75
- emitter life 163, 228
- emitter lifetime 164, 216
- emitter material 155
- emitter module 229
- emitter profiles 159–60, 163, 187
- emitter protrusion 85, 91
- emitter recession 160
- emitter research 5
- emitter shortening 162
- emitter temperature 35–36, 38, 45, 50, 59, 72–73, 159, 227
- emitter tip 4, 13–14, 40, 71, 155–57, 160, 178, 182, 188, 198, 212
- emitter tip geometry 224
- emitter tip profile 182
- emitter-extractor lens effect 140
- energy, adatom creation 179
- energy barriers 155, 162–63, 188, 190, 212, 230
- ESD, *see* electron-stimulated desorption
- extraction voltage 34–38, 59–60, 62–69, 71–73, 75–78, 85–86, 92–93, 96–98, 128–29, 138–40, 168–74, 176–77, 180–89, 191–93, 226–29
- extraction voltage axis 79
- extractor aperture 33–34, 36–38, 47, 54, 60, 142, 224, 229, 231, 238

- facet beam 5, 58, 107, 126–27,
 129, 143–45, 224, 238
 facet center 52, 56–57, 66–67, 69,
 71–73, 75–76, 100–4,
 125–28, 132–33, 165–66,
 176, 192, 208–9, 212,
 222–23
 facet collapse 210
 facet currents 49, 65, 91
 facet diameter 51, 71, 128, 183,
 187, 210
 facet edge 51–52, 62–63, 93, 106,
 160, 175, 182–84, 192,
 195–96, 200, 210, 222
 facet electrode 52
 facet emission 6, 46–47, 50, 59,
 93, 95
 facet emission pattern 49, 55,
 57–59, 71, 93, 164, 224,
 226–27, 231, 238
 facet extractor lens effect 72, 74
 facet geometry 150, 165, 167,
 176, 209, 225, 230
 facet instability 221
 facet launch position 57
 facet shape 82, 166
 facet size 69–71, 75, 165, 168,
 174, 178, 188, 192, 195,
 208–9, 212, 225, 229
 facet size adjustments 209
 faceting
 hill-and-valley 44
 thermodynamic 198
 Fermi energy 7–8, 10–11, 19,
 24–25, 81
 Fermi–Dirac distribution 11,
 22–23, 81
 field enhancement factor 67–68,
 76–77, 79–80, 87, 93,
 136–37, 141, 165, 176,
 235, 238
 field particles 122
 free-electron theory 9
 full width half maximum (FWHM)
 110, 112, 116, 130,
 134–35, 137–40, 193–95
 FWHM, *see* full width half
 maximum
 Gaussian intensity distribution
 115, 192
 Gaussian source intensity profile
 113
 geometrical stability 147–48, 150,
 152, 154, 156, 158, 160,
 162, 164, 166, 168, 170,
 172, 212, 222–24
 gun tilt setting 238
 Holtsmark regime 123–25, 140
 Holtsmarkian beam 127
 island atoms 201, 204, 207, 210
 Jansen’s equations 122, 124
 lens, facet extractor lens 50–53,
 55, 57–58, 108, 210
 monochromator 216–17
 multibeam systems 49, 145
 negative lens effect 52, 54
 negative lenses 54
 oxygen 5, 153, 183
 pencil beam 122–24, 127, 135
 pencil beam regime 127–28
 pure 123
 practical brightness 95–96,
 108–10, 112–16, 118–19,
 122, 133, 140, 143, 222,
 239
 probe electrons 96
 probe-forming systems 109, 111,
 113–14, 118, 239

- probe size 108, 111–12, 114, 118
 profile
 current 171, 203–4, 206–7,
 210–11
 electron-probe 111
 probe intensity 111–12, 142
 steady-state 158
 protrusion 42–43, 50, 69, 71–73,
 77, 84, 97, 100, 107, 125,
 143, 190, 192
 room-temperature 60, 62
 temperature-dependent 85,
 89
 pyrometer 39

 radiation losses 38, 41
 radiometry 109
 retarder element 135

 scanning electron microscopy
 (SEM) 31, 45, 60, 111,
 149, 216–17, 222, 224,
 226, 231
 scanning transmission electron
 microscopy (STEM) 208,
 216
 scanning tunneling microscopy
 (STM) 201
 Schottky effect 6, 16, 22, 195
 Schottky electron emitters 165,
 183, 190, 194
 commercial 73
 Schottky electron source 2, 6–7,
 12, 30, 35, 84, 86–87,
 138–39, 230
 Schottky emission 22–23, 76
 extended 23
 Schottky emission equation
 22–24
 analytical 78–79
 analytical extended 85, 88
 extended 23
 Schottky emitter cones 31

 Schottky emitter facet 178
 Schottky emitter geometry 28
 Schottky emitter gun 120
 Schottky emitter materials 9, 40
 Schottky emitter module, standard
 135
 Schottky emitter tips 149, 154
 Schottky emitters 3–6, 12–13, 15,
 29–32, 36–38, 42, 44–47,
 68–69, 121, 125–26,
 155–60, 163–64, 182–84,
 197–99, 221–22
 Schottky plots 50, 67, 75–77,
 79–80, 85, 93, 136, 176,
 224–25, 231
 Schottky source 3, 5, 25, 29–30,
 32, 38, 45, 49, 101, 114–15,
 134, 142, 230
 Schottky source module 26
 Schottky source performance 215
 Schottky sources distributions
 124
 Schotty emission 23
 Schrödinger equation 16–18, 20
 scintillator 33–34
 SEM, *see* scanning electron
 microscopy
 shank emission 36–37, 47, 78
 single-beam systems 145
 source image 95, 108–11, 113,
 115–16, 118, 217
 source image area 110
 source image plane 110
 source image size 108, 110, 112,
 116, 140, 216
 source intensity distribution 114
 source intensity profile 113, 115
 source-monitoring tools 224–25
 spatial beam coherence 140
 static emitter shape 216
 STEM, *see* scanning transmission
 electron microscopy
 STM, *see* scanning tunneling
 microscopy

- suppressor-emitter-extractor module 4
- suppressor voltage, constant 33, 37, 46–47, 59–60, 62, 65–66, 77–78, 90, 98, 105, 141, 160–61
- surface energy 152–53
- surface orientation 151
- surface tension 152, 157–60, 162, 196
- tangential energy 11, 26, 96–97, 100–4, 109, 114
- tangential energy distribution of electrons 27, 103
- thermionic emitters 113
- transmission electron microscope 2, 114
- transmission electron microscopy 95
- tungsten 9, 38–39, 41–42, 88–89, 148, 153, 160, 184
bare 12, 30, 153
- tungsten emitters 159
bare 160
- tungsten field emitters, single-crystalline 147
- tungsten surfaces 30
- Wulff construction 152
- Wulff plot 152–53, 167
- Wulff plot for Schottky emitter material 153
- YAG, *see* yttrium-aluminum-garnet yttrium-aluminum-garnet (YAG) 33, 85, 148, 191
- zirconium 5, 153, 183